EUROPEAN MECHANICAL SCIENCE

Research Article

e-ISSN: 2587-1110

Modeling and simulation of earth coverage of a low earth orbit (LEO) satellite

Murat Bakirci[1*]

[1]Faculty of Aeronautics and Astronautics, Tarsus University, Mersin 33400, Turkiye

Orcid: M. Bakirci (0000-0003-2092-1168)

Abstract: Efficient management of operations in near space, just beyond the Earth's atmosphere, relies on the precise control of satellites positioned relatively close to our planet. Satellite systems, serving critical functions in telecommunications, observation, exploration, and more, have demonstrated their prowess as a transformative technology, consistently delivering high-precision data over numerous years. Among satellite systems, Low Earth Orbit (LEO) technology is gaining prominence due to its advantages, including lower power requirements for transmission, reduced propagation delays, and heightened coverage for polar regions. Achieving optimal efficiency from LEO satellites necessitates a thorough understanding of their fundamental orbital parameters and precise control over them. This study explores the orbital analysis and Earth coverage considerations of LEO satellites, scrutinizing orbital parameters in detail to compute coverage areas across various scenarios. Through this investigation, the potential benefits of data exchange with ground stations facilitated by LEO satellites are explored. In addition, the implications are discussed regarding the adjustment of data exchange topologies according to geographical locations and country borders.

Keywords: LEO satellite, earth coverage, orbital parameters, ground track.

1. Intorduction

Satellite systems are one of the key components of space research and communication technologies due to the many advantages they provide. The most common usage areas of this technology can be listed as communication [1-4], observation [5], warfare applications [6], and positioning applications at various scales [7]. The importance of low-altitude satellites, which are used for purposes such as observation and exploration on Earth, is increasing over time. Satellites known as Low-Earth orbit (LEO) are reliable systems capable of meeting such requirements with sufficient accuracy [8-13]. In addition to all the other benefits, they have all the necessary features for positioning when GNSS satellites cannot be used effectively [9]. Since they are much closer to the Earth than GNSS satellites, the signals received from these satellites are much stronger [8]. Moreover, the orbital information of these satellites was made available to the public by the North American Aerospace Defense Command (NORAD), which greatly facilitated the work of the relevant researchers [14].

LEO satellites have found a myriad of applications across various domains, owing to their proximity to Earth and the advantages they offer in terms of data transmission, coverage, and responsiveness. One prominent application lies in telecommunications, where LEO satellites serve as vital components in global communication networks [15, 16]. These satellites facilitate voice and data communication services, including mobile phone calls, internet connectivity, and multimedia streaming. Due to their relatively low altitude, LEO satellites enable low-latency communication, making them particularly suitable for real-time applications such as voice calls and video conferencing [17]. Moreover, LEO satellite constellations, characterized by multiple satellites orbiting the Earth in close proximity, enhance network reliability and coverage, ensuring seamless connectivity even in remote or underserved regions [18]. Beyond traditional telecommunications, LEO satellites also play crucial roles in emergency communication systems, providing essential communication links during natural disasters, humanitarian crises, and remote rescue operations [19, 20]. Their rapid deployment capabilities and wide coverage areas make LEO satellites indispensable tools for emergency response and disaster management efforts worldwide.

*Corresponding author:
Email: muratbakirci@tarsus.edu.tr

Cite this article as:
Bakirci, M. (2024). Modeling and simulation of earth coverage of a low earth orbit (LEO) satellite. *European Mechanical Science*, *8*(2): 85-92. https://doi.org/10.26701/ems.1466031

History dates:
Received: 06.04.2024, *Revision Request*: 06.05.2024, *Last Revision Received*: 09.05.2024, *Accepted*: 23.05.2024

Another significant application of LEO satellites is in Earth observation and environmental monitoring [21]. Equipped with advanced sensors and imaging technologies, LEO satellites capture high-resolution imagery of the Earth's surface, atmosphere, and oceans [22, 23]. These satellites facilitate a wide range of applications, including weather forecasting, climate monitoring, disaster management, agriculture, and urban planning [24, 25]. By continuously monitoring environmental parameters such as weather patterns, sea surface temperatures, vegetation health, and land use changes, LEO satellites provide valuable data for scientific research, resource management, and policy-making. Furthermore, LEO satellite imagery aids in the assessment and mitigation of natural disasters such as hurricanes, floods, wildfires, and earthquakes by enabling early detection, rapid response, and post-event damage assessment [26]. The real-time monitoring capabilities of LEO satellites also contribute to environmental conservation efforts by tracking deforestation, pollution, and biodiversity loss, facilitating informed decision-making to address pressing environmental challenges [27].

Satellite systems, along with other unmanned systems, maintain continuous communication with ground stations, ensuring they are under constant supervision, regardless of whether they fulfill their duties proficiently or encounter issues. In this context, while updates are transmitted by ground stations at certain times, the received telemetry information is also subject to control [28-30]. For this to happen, the satellite must enter the line of sight of the ground station. However, even this alone is not enough for data exchange to be efficient. The quality of data exchange may also depend on antenna gain, network relay speed, and even geographical conditions [31-33]. LEO satellites, which are closer to the Earth than other satellite systems, move relatively faster in their orbits and therefore communication can be established from the ground stations for limited times. On the other hand, the duration of data exchange is primarily dependent on the orbital parameters and the geographical location of the ground control stations on Earth [34, 35]. Especially in critical Earth-observation missions, it is necessary to know the orbit information and coverage area of the satellite with high accuracy [36, 37]. This is an essential requirement for many important applications. In this study, the orbital characteristics of LEO satellites were investigated by considering the basic Kepler parameters and focused on the coverage areas throughout their orbits. Thus, a framework has been tried to be drawn about how and to what extent they can communicate with ground stations.

2. Methodology

In the numerical study, the two-line element set provided by the NORAD system are used as initial values. After the first computations are made with these initial values, the iterative process starts, and the necessary computations for each time step of the satellite are made as follows: First, using NORAD's data, the period of the satellite orbit, T, is computed as mean motion $T = 86400/\text{mean motion}$. Then, using this period value, the semi-major axis is computed as follows.

$$a = \sqrt[3]{\left(\frac{T}{2\pi}\right)^2 \Upsilon} \tag{1}$$

where Υ is the standard gravitational parameter and has an approximate value of $3.986004418 \times 10^{14} m^3 s^{-2}$ for Earth. With the eccentricity, e, and mean anomaly, M, values from NORAD, the eccentric anomaly, E, is computed as follows:

$$M = E - e \sin E \tag{2}$$

Using the same eccentricity and mean anomaly values, the true anomaly value, θ, can also be computed as follows:

$$\theta = 2 \tan^{-1}\left(\sqrt{\frac{1+e}{1-e}} \tan\frac{E}{2}\right) \tag{3}$$

The position vector, $\hat{\mathbf{p}}$, relative to the center of Earth is then computed as follows:

$$\hat{\mathbf{p}} = [p\cos\theta \quad p\sin\theta \quad 0]^T \tag{4}$$

In the computation of $\hat{\mathbf{p}}$, inclination, i, right ascension, Ω, and argument of periapsis, ω, values provided by NORAD are also used. The magnitude of the position vector given above can be expressed as follows:

$$p = \frac{a(1-e^2)}{1+e\cos\theta} \tag{5}$$

The following set of transformation equations is used to transform the position vector from the perifocal coordinate system to the equatorial coordinate system.

$$\xi_i = \cos\Omega\cos\omega - \sin\Omega\cos i\sin\omega \tag{6a}$$

$$\xi_j = \sin\Omega\cos\omega + \cos\Omega\cos i\sin\omega \tag{6b}$$

$$\xi_k = \sin i\sin\omega \tag{6c}$$

$$\zeta_i = -\cos\Omega\sin\omega - \sin\Omega\cos i\cos\omega \tag{7a}$$

$$\zeta_j = -\sin\Omega\sin\omega + \cos\Omega\cos i\cos\omega \tag{7b}$$

$$\zeta_k = \sin i\cos\omega \tag{7c}$$

$$\eta_i = \sin i\sin\Omega \tag{8a}$$

$$\eta_j = -\sin i\cos\Omega \tag{8b}$$

$$\eta_k = \cos i \tag{8c}$$

Each satellite will have different Keplerian element values and thus different altitudes and orbital trajectories. Altitude is a critical parameter that directly determines the orbital speed and coverage area. As the altitude increases, the width of the swath, which is a circular area, increases. However, considering the two-dimensional model, this coverage area, which is almost a full circle around the equator, will deviate from a circle and take on

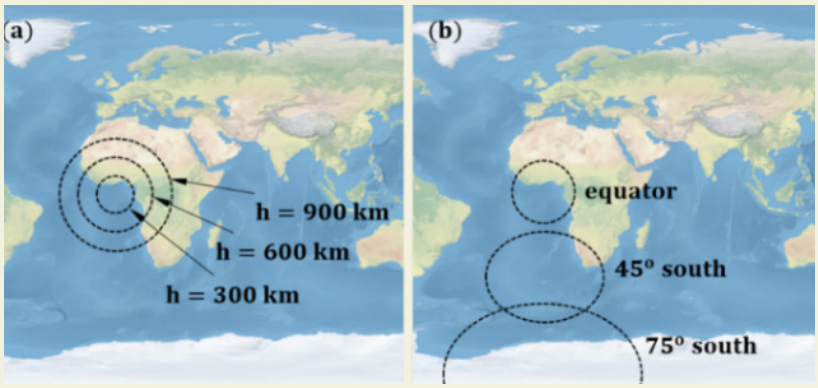

Figure 1. Variation of satellite coverage area with altitude (a) and latitude (b).

a different shape near the poles. Fig. 1a shows the variation of coverage area with satellite altitude. As shown in the figure, an increase of about 800% in the coverage area occurs when the altitude increases from 300 km to 900 km. Fig. 1b shows the different coverage areas of a 500 km altitude LEO satellite at different points on the Earth.

Some of the key orbital parameters of a LEO satellite in Earth orbit are given in Fig. 2. In the figure, r is the radius of the Earth, h is the altitude of the satellite, GS is the location of the ground station, s is the subsatellite point, σ is the satellite's coverage radius, τ is the projection of the satellite coverage angle relative to the Earth's center (C), δ is the angular distance between the ground station and the subsatellite point, ε is the elevation angle, and γ is the azimuth angle.

Based on the figure, the coverage radius of the satellite is determined as follows:

$$\sin\sigma = r/r + h \tag{9}$$

It must be noted that the angular relationship between σ and τ is $\sigma + \tau = 90^o$ as can be deduced from the figure. When the latitude, λ_s, longitude, φ_s, of the subsatellite point and the latitude, λ_{GS}, of the GS are known, the azimuth angle, γ, and the angular distance, δ, between these points are calculated as follows:

$$\cos\delta = \sin\lambda_s \sin\lambda_{GS} + \cos\lambda_s \cos\lambda_{GS} \cos\Delta\lambda \tag{10}$$

$$\cos\gamma = \frac{\sin\lambda_{GS} - \cos\delta\sin\lambda_s}{\sin\delta\cos\lambda_s} \tag{11}$$

where $\Delta\lambda$ is the angular distance between the subsatellite point and the ground station. Depending on whether the GS is east or west from the s, the azimuth angle will take values greater or less than 180 degrees.

Specifying Fig. 2 in more detail, additional parameters can be determined for the orbiting satellite. Fig. 3 shows the angular relationship between the satellite, GS, and subsatellite point s. Using the geometric figure, the angle of inclination of the satellite and the distance between the satellite and the GS can be computed as follows:

$$\tan\nu = \frac{\sin\sigma\sin\delta}{1 - \sin\sigma\cos\delta} \tag{12}$$

and the distance between the satellite and GS is

$$d = r(\sin\delta/\sin\nu) \tag{13}$$

where ν is the nadir angle, the angle between the subsatellite point and the GS, measured from the satellite to the GS. Using the obtained nadir angle, the elevation angle, ε, of the satellite is calculated as follows:

$$\cos\varepsilon = \sin\nu/\sin\sigma \tag{14}$$

When an LEO satellite is within the detection area of the GS, the primary factor that determines the data transfer time between the satellite and the GS is the satellite's inclination. While this time increases at high elevation angles, it decreases dramatically as the elevation decreases;

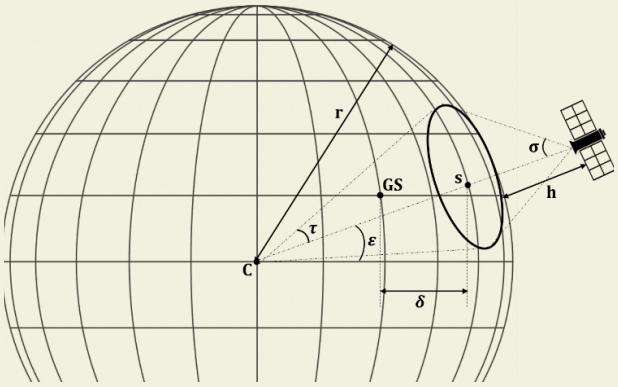

Figure 2. Orbital parameters of the LEO satellite.

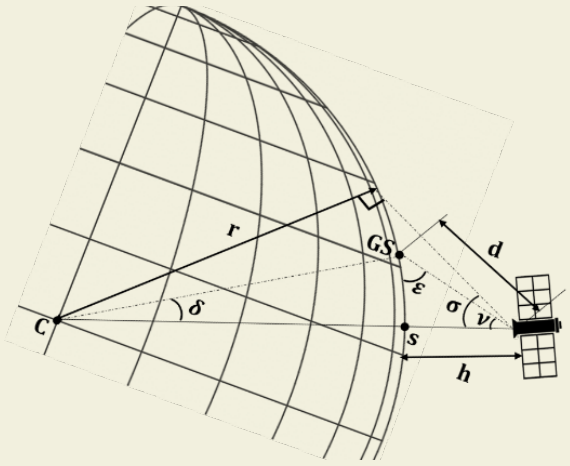

Figure 3. Different perspective of orbital parameters of the LEO satellite.

https://doi.org/10.26701/ems.1460031

that is, the data transfer time is a function of the elevation angle. When the satellite is at high elevation angles, the transfer time will be longer, as it will be in view of the GS for a longer period of time. At elevation angles below approximately 5 degrees, communication with the satellite cannot be established due to geographical constraints. The relationship between the elevation angle and the angular distance between the subsatellite point and GS can be expressed as follows.

$$\delta = \cos^{-1}\left(\frac{r}{r+h}\cos\varepsilon\right) - \varepsilon \tag{15}$$

Fig. 4 shows the variation of elevation angle, ε, with angular distance, δ, between the subsatellite point and GS for LEO satellites with different altitudes. As can be seen from the graph, the elevation angle affects the communication time significantly due to the change in the angular distance between the subsatellite point and GS.

3. Results

Simulations were performed using the set of operations described in the previous section, utilizing the NORAD dataset as initial values. Considering that the true anomaly value is a function of time, eccentric anomaly values are computed for each time stamp with true anomaly values calculated using the initial value. This approach allows for obtaining the position of the LEO satellite in time in the equatorial coordinate system.

However, another critical point to consider is the Earth's rotation. So far, computations for the satellite have taken into account only the motion of the satellite. However, since the Earth's rotation will affect all computations, they must be adjusted accordingly. Only through this adjustment can the trajectory of the satellite over the rotating Earth be accurately determined. To achieve this, the position vector obtained in (4) must be corrected, taking into account the angular velocity of the Earth, as follows:

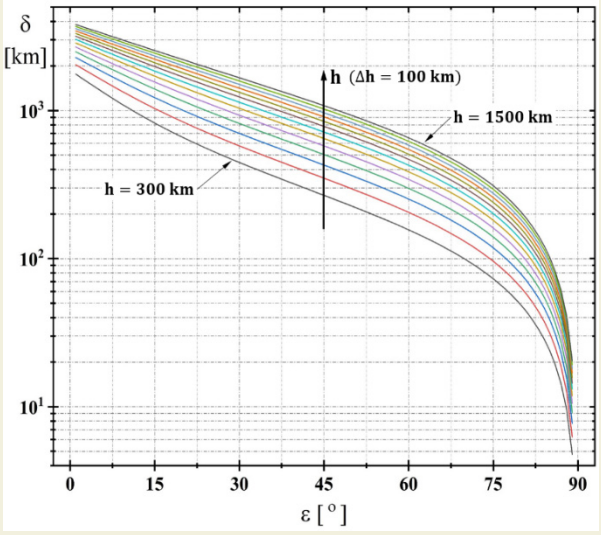

Figure 4. Variation of elevation angle with angular distance between subsatellite point and GS for different altitudes.

$$\hat{\mathbf{p}}_{cor} = R_{e,t} \times [p\cos\theta \quad p\sin\theta \quad 0]^T \tag{16}$$

where $\hat{\mathbf{p}}_{cor}$ indicates corrected position matrix and $R_{e,t}$ is the angular velocity matrix of the Earth and is expressed as

$$R_{e,t} = \begin{bmatrix} \cos(\omega_e t) & \sin(\omega_e t) & 0 \\ -\sin(\omega_e t) & \cos(\omega_e t) & 0 \\ 0 & 0 & 1 \end{bmatrix} \tag{17}$$

where ω_e is the angular velocity of the Earth. The subsatellite point of the LEO satellite can be easily found by subtracting the Earth radius from the altitude of the satellite.

Thus, the correct position vector, $\hat{\mathbf{p}}_{cor}$, of the considered satellite is obtained. From here, the actual coordinates of the subsatellite point on Earth are computed as follows

$$\lambda_s = \sin^{-1}(p_z/r) \tag{18}$$

$$\varphi_s = \cos^{-1}\left(\frac{p_x}{r\cos\lambda_s}\right) \tag{19}$$

where p_x and are the x and z components of the corrected position vector, $\hat{\mathbf{p}}_{cor}$, respectively. Now that the correct coordinates of the satellite have been obtained, it remains to compute whether or not the GS is within the satellite's coverage area. Since the coordinates of both the subsatellite point and GS are known, and the distance between inter-latitude is also known, using (10), the distance between the subsatellite point and GS is determined, and by normalizing the coverage area with the distance between inter-latitudes, the maximum distance to be covered by the satellite is computed as follows.

$$\vartheta = 2\tau r \tag{20}$$

Fig. 5 shows the ground track map illustrating a full orbit of an LEO satellite around the Earth. The parameters used in this orbital simulation are as follows: eccentricity is 0.2, semimajor axis is 8000 km, true anomaly is 70 degrees, inclination is 70 degrees, argument of perigee is also 70 degrees, and right ascension is 120 degrees. Using these parameters, the orbital characteristics were computed as follows: the initial radius is 7188 km, initial velocity is 7.815 km s^{-1}, angular momentum is 55329 km^2 s^{-1}, mean anomaly is 0.866 rad, eccentric anomaly is 1.039 rad, perigee radius is 6400 km, flight path angle is 0.174 rad, and energy is -24.913 km^2 s^{-2}.

In Fig. 6, the velocity and position vector components corresponding to this orbital motion are provided. In both graphs, the variations of the velocity vector and position vector with respect to true anomaly are given. Based on the velocity-true anomaly graph, the average velocity of the satellite during its orbital motion is 7.326 km s^{-1}, and their minimum and maximum velocities are 5.777 km s^{-1} and 8.714 km s^{-1}, respectively. Fig. 7 shows the variation of the same velocity and position vector components with respect to time.

In Fig. 8a, the orbital motion of the satellite around the

Earth is expressed in 3D. Similarly, the velocity variation along the orbital motion is given in Fig. 8b. Note that in this graph, different vector lengths correspond to different magnitudes of velocity.

Fig. 9a and Fig. 9b show a ground track map illustrating 5 and 43 orbits of an LEO satellite around the Earth, respectively. For both simulations, all orbital parameters are the same except their periods. The orbital motion period in Fig. 9b is five times shorter, which provides a general framework for most LEO satellites, considering their high-speed orbital motion.

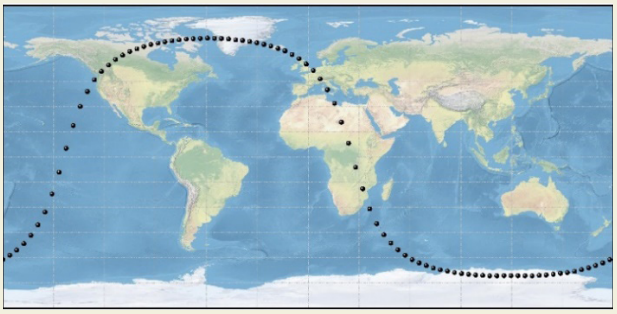

Figure 5. Ground track for the LEO satellite.

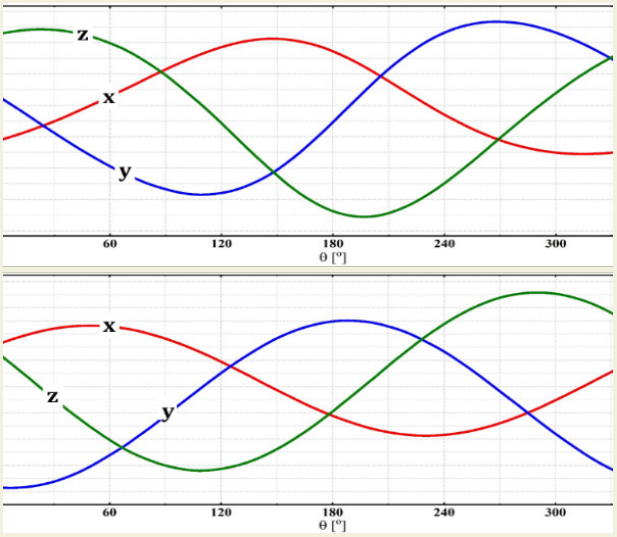

Figure 6. Variation of position and velocity vector components with respect to true anomaly.

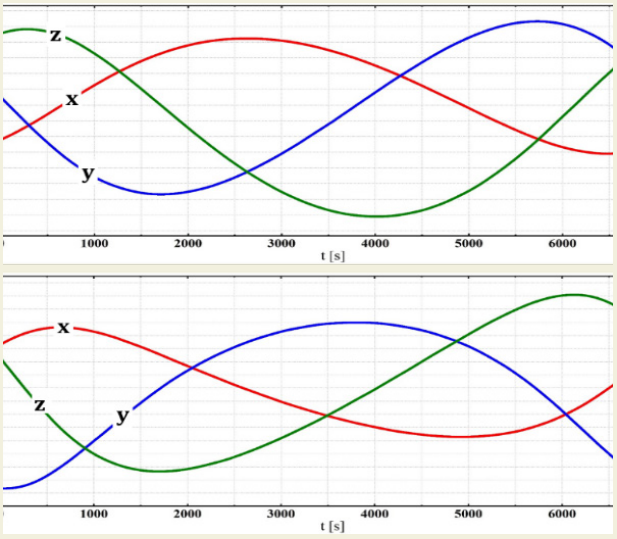

Figure 7. Variation of position and velocity vector components with respect to time.

Table 1 shows the numerical values corresponding to the azimuth and elevation angle diagram obtained from the numerical study. In this simulation, the GS was assumed to be located at the point on the Earth corresponding to 0 latitude and longitude. On the other hand, the LEO satellite corresponding to Fig. 9b, was assumed to have a 70-degree inclination, at an altitude of 750 km, and to make 43 complete orbits around the Earth each day.

In the table, the position of the GS is expressed as the center, that is, the point where the zero values intersect. At this point, the elevation angle is maximum, that is, 90 degrees. As you go from the center of the table, the elevation angle decreases. When horizontal angle values are considered as x components and vertical angle values as y components, the azimuth value is 0 at the intersection of 0 and [90,80), and is 90 at the intersection of (80,90] and 0, and is 180 at the intersection of 0 and (-80,90], and is 270, at the intersection of [-90,80) and 0. All cells

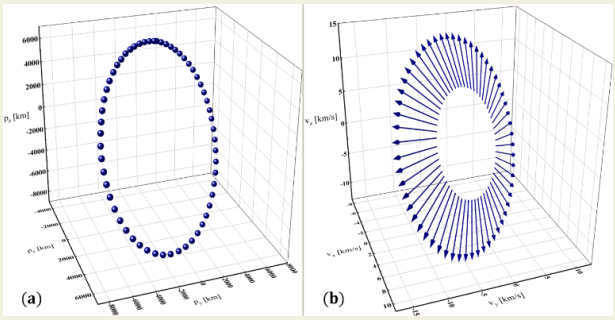

Figure 8. Three dimensional illustration of the LEO satellite's orbital motion around the Earth (a), and velocity variation along the orbital motion (b).

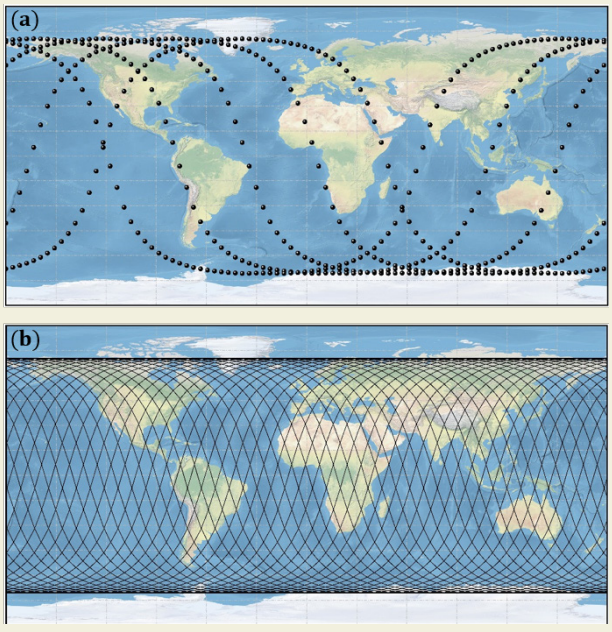

Figure 9. Ground track of 5 (a) and 43 (b) orbits of the LEO satellite.

https://doi.org/10.26701/ems.1460031

Table 1. Satellite and GS communication instants.

	[°]																		
[°]	[-90, -80)	[-80, -70)	[-70, -60)	[-60, -50)	[-50, -40)	[-40, -30)	[-30, -20)	[-20, -10)	[-10, 0)	0	(0, 10]	(10, 20]	(20, 30]	(30, 40]	(40, 50]	(50, 60]	(60, 70]	(70, 80]	(80, 90]
[90, 80)	-	-	-	-	-	-	1,2,6	2	4,11		9	5,9	-	8,12	-	-	-	-	-
[80, 70)	-	-	-	3	1,5	1,2,6	2,4	4	11		11	5,9	9	12	8,10	-	-	-	-
[70, 60)	-	-	3	1,3,5	1,2,5	2,4,6	4	-	-		11	11,13	9	9,12	12	8,10	-	-	-
[60, 50)	-	-	1,3	1,2,5	2	4,6	-	-	-		-	11,13	-	9	9,12	8,10	10	7	-
[50, 40)	-	1,3	1,2,3	2,5	4	4,6	-	-	-		-	11,13	11	-	9,12	8,9	8,10	7	-
[40, 30)	-	1,3	2,5	-	4,6	-	-	-	-		-	13	11	-	12	9,12	8,10	7	-
[30, 20)	1	1,2,3	2,5	4	6	-	-	-	-		-	13	11	11	-	9,12	10	8	7
[20, 10)	1	2,3	5	4	6	-	-	-	-		13	-	-	11	-	12	9,10	8	7
[10, 0)	1	2,3	5	4	6	-	-	-	-		13	-	-	11	-	12	9	8,10	7
0																			
(0, -10]	1	2,3	4,5	4	-	6	-	-	-		13	-	-	11	11	12	9	8,10	7
(-10, -20]	1	2,3	4,5	-	-	6	-	-	-		13	-	-	-	11,12	12	9,10	-	7,8
(-20, -30]	1	2,3	4,5	-	-	6	-	-	13		13	-	-	-	11,12	-	9,10	-	7,8
(-30, -40]	-	2,3	3,4	4,5	-	6	-	-	13		-	-	-	-	11,12	-	9,10	7,8	7
(-40, -50]	-	2	3	4,5	-	-	6	-	13		-	-	-	12	11,12	10	9,10	7,8	-
(-50, -60]	-	2	3	4,5	5	-	6	-	13		-	-	-	12	11	10	9	-	-
(-60, -70]	-	-	3	3,4	5	5	-	6,13	13		-	-	12	12	10,11	9,10	9	-	-
(-70, -80]	-	-	-	3	-	5	-	6,13	6		-	12	12	10,11	10	-	-	-	-
(-80, -90]	-	-	-	-	-	-	5	13	6		6,12	12	-	10,11	-	-	-	-	-

with numerical values indicate communication times. In only 15 of the 43 full orbits made by the LEO satellite, the GS has entered the satellite's coverage area. As only 13 of them have the minimum elevation angle possible to communicate, they are listed in the table. In the other two cases, it will not be possible to establish a connection due to geographical constraints.

4. Conclusion

Despite having all the advantages, it is quite critical to know basic orbital parameters with high accuracy and to control them precisely in order to get the maximum efficiency from LEO satellites. For that reason, their ground tracks must be obtained with high accuracy, and communication instants with ground stations must be accurately calculated. The orbital analysis of a LEO satellite and the Earth coverage problem was investigated in this study. By computing the Keplerian parameters of the satellite, detailed orbital analysis was performed, and the orbital motion was determined for different inputs. By computing the position and velocity vectors, the changes in all phases of the trajectory were examined. Moreover, the coverage area, which indirectly depends on time, was obtained during its entire orbital motion, and it was computed when it exchanged data with the ground station. It was determined that a LEO satellite with specific orbital parameters is able to communicate in only 13 of the 43 orbits made in total. Satellite ground tracks have been analyzed in detail, and insight was gained about what topology should be planned for maximizing the communication time. It was concluded that a single LEO satellite can be used quite efficiently by establishing the optimum number of ground station networks at the proper locations of the Earth. Since Turkey, the area of interest in this study, has an approximately rectangular geographical shape, it will be sufficient to establish two ground stations, one in the east and another in the west, along the central axis of the territory.

Research Ethics

Ethical approval not required.

Author Contributions

The author(s) accept full responsibility for the content of this article and have approved its submission.

Competing Interests

The author(s) declare that there are no competing interests.

Research Funding

Not reported.

Data Availability

Not applicable.

Rererences

[1] Khalife, J.J., Kassas, Z.M. (2019). Receiver design for Doppler positioning with LEO satellites. *ICASSP 2019 - 2019 IEEE International Conference on Acoustics, Speech and Signal Processing*, 5506-5510. https://doi.org/10.1109/ICASSP.2019.8682554

[2] Bakirci, M., Cetin, M. (2022). Utilization of a vehicle's on-board diagnostics to reduce GPS-sourced positioning error. *2022 Innovations in Intelligent Systems and Applications Conference (ASYU)*, Antalya, Turkey, 1-4. https://doi.org/10.1109/ASYU52992.2022.9833873

[3] Cluzel, S., Franck, L., Radzik, J., Cazalens, S., Dervin, M., Baudoin, C. (2018). 3GPP NB-IOT coverage extension using LEO satellites. *2018 IEEE 87th Vehicular Technology Conference (VTC Spring)*, 1-5. https://doi.org/10.1109/VTCSpring.2018.8417874

[4] Su, Y., Liu, Y., Zhou, Y., Yuan, J., Cao, H., Shi, J. (2019). Broadband LEO satellite communications: architectures and key technologies. *IEEE Wireless Communications*, 26(2), 55-61. https://doi.org/10.1109/MWC.2019.8684206

[5] Crisp, N.H., Roberts, P.C.E., Livadiotti, S., Oiko, V.T.A., Edmondson, S., Haigh, S.J. (2020). The benefits of very low earth orbit for earth observation missions. *Progress in Aerospace Sciences*, 117, 1-18. https://doi.org/10.1016/j.paerosci.2020.100619

[6] Routray, S.K., Javali, A., Sahoo, A., Sharmila, K.P., Anand, S. (2020). Military applications of satellite based IoT. *2020 Third International Conference on Smart Systems and Inventive Technology (ICSSIT)*, 122-127. https://doi.org/10.1109/ICSSIT48917.2020.9214165

[7] Li, B., Ge, H., Ge, M., Nie, L., Shen, Y., Schuh, H. (2019). LEO enhanced global navigation satellite system (LeGNSS) for real-time precise positioning services. *Advances in Space Research*, 63(1), 73-93. https://doi.org/10.1016/j.asr.2018.08.026

[8] Khalife, J., Neinavaie, M., Kassas, Z.M. (2020). Navigation with differential carrier phase measurements from megaconstellation LEO satellites. *2020 IEEE/ION Position, Location and Navigation Symposium (PLANS)*, Portland, Oregon, 1393-1404. https://doi.org/10.1109/PLANS46316.2020.9110165

[9] Morales, J., Khalife, J., Kassas, Z.M. (2019). Simultaneous tracking of Orbcomm LEO satellites and inertial navigation system aiding using Doppler measurements. *2019 IEEE 89th Vehicular Technology Conference (VTC2019-Spring)*, 1-6. https://doi.org/10.1109/VTCSpring.2019.8746340

[10] Reid, T., Neish, A., Walter, T., Enge, P. (2018). Broadband LEO constellations for navigation. *NAVIGATION, Journal of the Institute of Navigation*, 65(2), 205-220. https://doi.org/10.1002/navi.249

[11] Lawrence, D., Cobb, H., Gutt, G., O'Connor, M., Reid, T., Walter, T. (2017). Navigation from LEO: current capability and future promise. *GPS World Magazine*, 28(7), 42-48.

[12] Chen, X., Wang, M., Zhang, L. (2016). Analysis on the performance bound of Doppler positioning using one LEO satellite. *IEEE Vehicular Technology Conference (VTC-Fall)*, 1-5. https://doi.org/10.1109/VTCFall.2016.7881273

[13] Kozhaya, S.E., Haidar-Ahmad, J.A., Abdallah, A.A., Kassas, Z.M., Saab, S.M. (2021). Comparison of neural network architectures for simultaneous tracking and navigation with LEO satellites. *34th International Technical Meeting of the Satellite Division of the Institute of Navigation (ION GNSS+ 2021)*, St. Louis, Missouri, 2507-2520. https://doi.org/10.33012/2021.17811

[14] North American Aerospace Defense Command (NORAD). "Two-line element sets." celestrak.com. https://www.celestrak.com/NORAD/elements/ (accessed Jan. 3, 2024).

[15] Geng, S., Liu, S., Fang, Z., Gao, S. (2020). An optimal delay routing algorithm considering delay variation in the LEO satellite communication network. *Computer Networks*, 173, 107166. https://doi.org/10.1016/j.comnet.2020.107166

[16] Ge, H., Li, B., Nie, L., Ge, M., Schuh, H. (2020). LEO constellation optimization for LEO enhanced global navigation satellite system (LeGNSS). *Advances in Space Research*, 66(3), 520-532. https://doi.org/10.1016/j.asr.2019.04.008

[17] Sun, X., Han, C., Chen, P. (2017). Precise real-time navigation of LEO satellites using a single-frequency GPS receiver and ultra-rapid ephemerides. *Aerospace Science and Technology*, 67, 228-236. https://doi.org/10.1016/j.ast.2017.03.008

[18] Lin, X., Chen, Y., Xue, J., Zhang, B., He, L., Chen, Y. (2024). Large-volume LEO satellite imaging data networked transmission scheduling problem: Model and algorithm. *Expert Systems with Applications*, 249(B), 123649. https://doi.org/10.1016/j.eswa.2023.123649

[19] Denis, G., de Boissezon, H., Hosford, S., Pasco, X., Montfort, B., Ranera, F. (2016). The evolution of Earth Observation satellites in Europe and its impact on the performance of emergency response services. *Acta Astronautica*, 127, 619-633. https://doi.org/10.1016/j.actaastro.2016.06.019

[20] Lourenço, R.B.R., Figueiredo, G.B., Tornatore, M., Mukherjee, B. (2019). Data evacuation from data centers in disaster-affected regions through software-defined satellite networks. *Computer Networks*, 148, 88-100. https://doi.org/10.1016/j.comnet.2018.11.022

[21] Pardini, C., Anselmo, L. (2020). Environmental sustainability of large satellite constellations in low earth orbit. *Acta Astronautica*, 170, 27-36. https://doi.org/10.1016/j.actaastro.2020.01.014

[22] Bakirci, M., Bayraktar, I. (2024). Transforming aircraft detection through LEO satellite imagery and YOLOv9 for improved aviation safety. *2024 26th International Conference on Digital Signal Processing and its Applications (DSPA)*, Moscow, Russian Federation, 1-6. https://doi.org/10.1109/DSPA.2024.9832371

[23] Bakirci, M., Bayraktar, I. (2024). Boosting aircraft monitoring and security through ground surveillance optimization with YOLOv9. *2024 12th International Symposium on Digital Forensics and Security (ISDFS)*, San Antonio, TX, USA, 1-6. https://doi.org/10.1109/ISDFS.2024.9832372

[24] Nwankwo, V.U.J., Chakrabarti, S.K. (2018). Effects of space weather on the ionosphere and LEO satellites' orbital trajectory in equatorial, low and middle latitude. *Advances in Space Research*, 61(7), 1880-1889. https://doi.org/10.1016/j.asr.2017.10.022

[25] Lele, N., Nigam, R., Bhattacharya, B.K. (2021). New findings on impact of COVID lockdown over terrestrial ecosystems from LEO-GEO satellites. *Remote Sensing Applications: Society and Environment*, 22, 100476. https://doi.org/10.1016/j.rsase.2021.100476

[26] Maiti, M., & Kayal, P. (2024). Exploring innovative techniques for damage control during natural disasters. *Journal of Safety Science and Resilience*, 5(2), 147-155. https://doi.org/10.1016/j.jssr.2024.02.005

[27] Numbere, A. O. (2022). Application of GIS and remote sensing towards forest resource management in mangrove forest of Niger Delta. *Natural Resources Conservation and Advances for Sustainability*, 433-459. https://doi.org/10.1016/j.nrsca.2022.05.015

[28] Salcedo, D. A., Ciafardini, J. P., & Bava, J. A. (2020). Antenna for telemetry data relay communications in LEO satellites and inmarsat-F4 constellation. In *2020 IEEE Congreso Bienal de Argentina (ARGENCON)* (pp. 1-6). IEEE. https://doi.org/10.1109/ARGENCON49523.2020.9505352

[29] Zhan, Y., Wan, P., Jiang, C., Pan, X., Chen, X., & Guo, S. (2020). Challenges and solutions for the satellite tracking, telemetry, and command system. *IEEE Wireless Communications*, *27*(6), 12-18. https://doi.org/10.1109/MWC.2020.9265056

[30] Stock, G., Fraire, J. A., Mömke, T., Hermanns, H., Babayev, F., & Cruz, E. (2020). Managing fleets of LEO satellites: Nonlinear, optimal, efficient, scalable, usable, and robust. *IEEE Transactions on Computer-Aided Design of Integrated Circuits and Systems*, *39*(11), 3762-3773. https://doi.org/10.1109/TCAD.2020.3021567

[31] Done, A., Lesanu, C., Căilean, A., Graur, A., & Dimian, M. (2017). Implementation of an on-line remote control ground station for LEO satellites. In *2017 21st International Conference on System Theory, Control and Computing (ICSTCC)* (pp. 855-859). IEEE. https://doi.org/10.1109/ICSTCC.2017.8107123

[32] Xia, D., Zheng, X., Duan, P., Wang, C., Liu, L., & Ma, H. (2019). Ground-station based software-defined LEO satellite networks. In *2019 IEEE 25th International Conference on Parallel and Distributed Systems (ICPADS)* (pp. 687-694). IEEE. https://doi.org/10.1109/ICPADS47876.2019.00099

[33] Done, A., Căilean, A., Leşanu, C., Dimian, M., & Graur, A. (2017). Considerations on ground station antennas used for communication with LEO satellites. In *2017 International Symposium on Signals, Circuits and Systems (ISSCS)* (pp. 1-4). IEEE. https://doi.org/10.1109/ISSCS.2017.8034928

[34] Done, A., Căilean, A., Leşanu, C., Dimian, M., & Graur, A. (2017). Design and implementation of a satellite communication ground station. In *2017 International Symposium on Signals, Circuits and Systems (ISSCS)* (pp. 71-75). IEEE. https://doi.org/10.1109/ISSCS.2017.8034929

[35] Zeng, T., Sui, L., Jia, X., Lv, Z., Ji, G., & Dai, Q. (2019). Validation of enhanced orbit determination for GPS satellites with LEO GPS data considering multi ground station networks. *Advances in Space Research*, *63*(9), 2938-2951. https://doi.org/10.1016/j.asr.2019.01.020

[36] Talgat, A., Kishk, M. A., & Alouini, M. S. (2021). Stochastic geometry-based analysis of LEO satellite communication systems. *IEEE Communications Letters*, *25*(8), 2458-2462. https://doi.org/10.1109/LCOMM.2021.3064457

[37] Meng, Y., Bian, L., Han, L., Lei, W., Yan, T., & He, M. (2018). A global navigation augmentation system based on LEO communication constellation. In *2018 European Navigation Conference (ENC)* (pp. 65-71). IEEE. https://doi.org/10.1109/EURONAV.2018.8443173